COMMUNICATION

ChemComm
www.rsc.org/chemcomm

Layer-by-layer self-assembled multilayers of redox polyelectrolytes and gold nanoparticles†

Nancy Ferreyra,[a] Liliane Coche-Guérente,[a] Julien Fatisson,[a] Manuel Lopez Teijelo[b] and Pierre Labbé*[a]

[a] *Laboratoire d'Electrochimie Organique et de Photochimie Rédox, UMR CNRS 5630, Institut de Chimie Moléculaire de Grenoble, FR CNRS 2607, Université Joseph Fourier, BP 53, 38041 Grenoble cédex 09, France. E-mail: Pierre.Labbe@ujf-grenoble.fr; Fax: +33 4 76514267; Tel: +33 4 76514718*

[b] *INFIQC, Departamento de Fisicoquímica, Facultad de Ciencias Químicas, Universidad Nacional de Córdoba, Pabellón Argentina, Ciudad Universitaria, 5000 Córdoba, Argentina. E-mail: mlopez@mail.fcq.unc.edu.ar; Fax: +54 351 4334188; Tel: +54 351 4334169*

Received (in Cambridge, UK) 15th May 2003, Accepted 23rd June 2003
First published as an Advance Article on the web 9th July 2003

Construction and characterization of structural and charge transport properties of electrostatically LbL self-assembled multilayers of gold nanoparticles and a viologen-based redox-active polyelectrolyte is reported.

Nanoparticles based nanostructured films are currently under intense investigation since they offer the potential for applications in various fields such as semiconductors, molecular electronics, photovoltaic, chemical and biological sensing and catalysis.[1] The assembly of metal nanoparticles into bi- or tridimensional superstructures has been reported using various kinds of electroactive linkers such as dithiols/bipyridinium,[2] thionine[3] or carboxylate/metal cation (Cu^{2+})/carboxylate,[4] which allowed the tailoring of nanoengineered architectures with novel electronic properties.

Recently the layer-by-layer (LbL) growth of polyelectrolyte/gold nanoparticle films has also been reported[5–8] using the electrostatic method popularised by Decher.[9] These works have demonstrated that depending on the polyelectrolyte structure and nanoparticle morphology as well as conditions of self-assembling, the final properties of charge transport and permeability within the assembly can be varied from a film with bulk metal conductivity[5] to a film exhibiting electronic charge transport from electrode through the film *via* an electron hopping from nanoparticle to nanoparticle. A tunable mobility of electrolyte ions moving through the film (necessary for electroneutrality) has also been described.[8] On the other hand, it has been also demonstrated that electronic charge transport within LbL self-assembled multilayers of polyelectrolytes can occur by electron hopping between adjacent molecular redox centers that are covalently grafted on the polyelectrolyte backbone. Such systems involved redox polyelectrolytes assemblies such as poly(butanylviologen)/poly(styrenesulfonate),[10] poly(allylamine)ferrocene or osmium complex-derivatized poly(allylamine)/glucose oxidase[11,12] or viologen-functionalized poly(vinylpyridinium)/nitrate reductase.[13]

To date, LbL multilayer superlattices of metallic nanoparticles and redox polyelectrolytes has not yet been reported, and for the first time in this communication, we describe the electrostatic LbL assemblies of negatively charged gold nanoparticles (NP) of two different sizes with the viologen-based cationic redox polyelectrolyte (PV)[13] (ESI)†.

The assembling procedure was realized on clean surfaces using either quartz slides that were negatively charged by activation in a basic medium or gold electrodes (d = 2 mm) that were first modified with 3-mercapto-1-propane-sulfonic acid (MPS). The first layer of PV was assembled by dipping the surface in an aqueous solution of PV (1 mg mL^{-1}) in 0.1 M phosphate buffer (pH 7.5) for 15 min and then extensively rinsing with pure buffer solution. The resulting surface was then transferred into a well-defined colloid of gold nanoparticles (NP_6: 6.4 ± 0.6 nm and NP_{11}: 11.0 ± 0.7 nm)[14] for 15 min and again extensively rinsed with pure buffer. Alternate contact with PV solution and NP colloid allowed the generation multilayered structures that were further *in situ* characterized using UV-visible absorption spectroscopy, ellipsometry and cyclic voltammetry.

The growing of multilayered PV-NP assemblies on a quartz slide was unambiguously demonstrated from UV-visible absorption experiments. As shown in Fig. 1A (spectra (a) and (c)), NP_{11} adsorption only occurs once the quartz surface has been modified by adsorption of a first PV layer. The resulting $(PV\text{-}NP_{11})_1$ assembly exhibits an UV-visible absorption band with λ_{max} = 527 nm, which is attributed to the surface plasmon resonance absorption band of Au nanoparticles.[15] Comparison with the absorption spectrum of the native NP_{11} gold colloid (spectrum (b) of Fig. 1A) indicates that the nanoparticles keep their integrity within the assembly while the red shift from 516 to 527 nm can be attributed to change in dielectric environment.[15] Similar conclusions could be obtained using NP_6 colloids (not shown). The growing of multilayered PV-NP assemblies on quartz slides was evidenced from the stepwise increase of the NP_6 or NP_{11} surface plasmon resonance absorption band intensity (Fig. 1B). The observed linear increase in absorbance shows that each dipping cycle deposits roughly the same amount of nanoparticles. This amount could be estimated to be 1.3×10^{11} and 1.6×10^{11} nanoparticles cm^{-2} respectively for each layer of NP_6 or NP_{11} (ESI)†. The PV-NP multilayer assemblies exhibited excellent stability as evidenced by the absence of significant change in absorption spectra after storing the films for 72 hours in contact with phosphate buffer.

Ellipsometry was also used to follow step by step the growth of a $(PV\text{-}NP_6)_n$ assembly on MPS-thiolated gold surfaces. The Δ-ψ trajectories obtained at two wavelengths (546.1 and 632.8

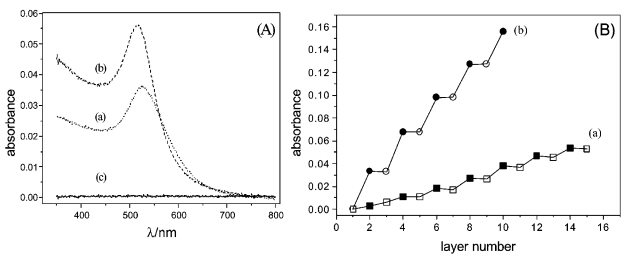

Fig. 1 A: Absorption spectra of (a) $(PV\text{-}NP_{11})_1$ assembly in 0.1 M phosphate buffer, pH 7.5 and (b) of the NP_{11} Au colloid (l = 0.1 cm). Spectrum (c) represents the absorption spectrum of the quartz slide after contact with the NP_{11} colloid without a previous adsorption of PV. B: Plot of the maximal absorbance of a PV-NP assembly grown on a quartz slide as a function of the layer number for (a) NP_6 (λ_{max} = 544 nm) and (b) NP_{11} (λ_{max} = 534 nm) nanoparticles, open and closed symbols are respectively related to the PV and NP top layer.

† Electronic supplementary information (ESI) available: see http://www.rsc.org/suppdata/cc/b3/b305347d/

DOI: 10.1039/b305347d

nm) for assemblies ended either by PV or NP were fitted on the basis of a single layer of isotropic optical properties. The best fits yield values of the complex refractive index ($\hat{n}$)[12] of 1.438–0.015i and $\hat{n}$ = 1.439–0.019i for PV and NP ended assemblies respectively. The mean thickness determined from the fits is presented as a function of layer number in Fig. 2. The results show that PV adsorption does not contribute to the thickness change while for each NP layer a 4.4 ± 0.5 nm increase of the thickness is observed on average, which is smaller than the 6.4 nm diameter of the NP_6 nanoparticles. This implies a substantial overlap between adjacent Au layers. The refractive index of the film is very different from that of bulk gold ($\hat{n}$ = 0.197–3.45i)[16] as well as of superlattices made of gold nanoparticles and 1,4-benzenedimethanethiol linkers ($\hat{n}$ = 2.4–1.38i)[16] but very similar to hydrated multilayer film of pure organic material.[12] This demonstrates that the as-prepared and *in situ* characterized PV-NP assemblies should be strongly hydrated.

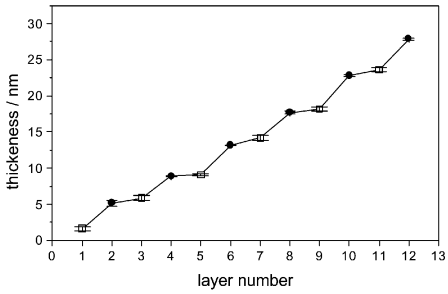

Fig. 2 Ellipsometric thickness evolution of a PV-NP_6 multilayer film as a function of layer number. (□) and (●) are respectively related to the PV and NP top layer. *In situ* ellipsometric measurements were realized in 0.1M phosphate buffer (pH 7.5).

Fig. 3A shows cyclic voltammograms (CVs) recorded for each adsorbed layer of an Au/MPS/(PV-NP_6)$_n$PV modified electrode. Up to a scan rate of 0.200 V s^{-1} the CVs exhibit a thin layer behaviour with reasonably symmetric peaks at E'° = −0.460 V and peak height proportional to scan rate, which is indicative of a rapid electron transfer from the underlying gold

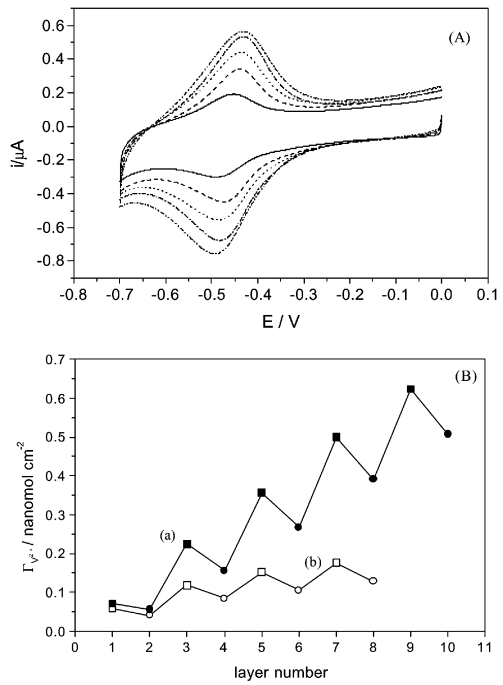

Fig. 3 (A) Cyclic voltammetry (100 mV s^{-1}) of Au/MPS/(PV-NP)$_n$PV electrodes as a function of *n*. (B) Evolution of surface coverage of electroactive viologen moieties in a Au/MPS/(PV-NP) assembly for (a) NP_6 and (b) NP_{11} nanoparticles as a function of layer number. (□) and (●) are respectively related to the PV and NP top layer.

electrode to successive PV-NP bilayers. Similar behaviour was observed for the Au/MPS/(PV-NP_6)$_n$ where the top layer was constituted of gold nanoparticles. The surface coverage of electroactive viologen center, obtained from the analysis of the linear part of the peak height evolution *versus* potential scan rate, is presented in Fig. 3B as a function of layer number for PV and NP_6 (curve (a)) or NP_{11} (curve (b)). There is a significant decrease in the percentage of redox active viologen on adsorption of the NP layer. However, a steady increase in the amount of redox active viologen on the electrode for each successive PV-NP added bilayer is observed. This behavior is similar to the one already observed in multilayers of glucose oxidase with poly(allylamine)ferrocene.[11] Electrostatic interaction of anionic NP with cationic PV should provide at least two different viologen environments within the film, one of them being inaccessible to electron transfer. Fig. 3B also shows for lower NP size a higher surface coverage of electroactive viologen. As the NP size increases, it should be expected that, within the multilayer, the electron transfer between two successive PV layers sandwiching a NP layer becomes more and more difficult as a consequence of a bigger distance between viologen centers. This behaviour also suggests that electron transport within the PV-NP multilayer mainly occurs by an electron hopping process between adjacent redox groups whereas electron transfer from viologen to nanoparticle as well as from nanoparticle to nanoparticle should not be an efficient process. Similar conclusions could be obtained at higher NP surface coverage per layer (ESI†). This result strongly contrasts with previous results that reported bulk metal conductivity[5] or interparticle electron hoping.[8] Work is in progress to elucidate these differences in particular by studying the influence of self-assembling conditions such as ionic strength, intermediate rinsing, drying and rehydrating steps. Indeed, it has been recognized that important reorganization of electrostatically self-assembled multilayers can occur not only with time, but also depending on the conditions of storing and assembling. The control of these parameters appears to constitute a key step for the design of new materials with reproducible and adaptative properties.

Dr Erica Forzani is gratefully acknowledged for helpful discussions and collaboration in performing ellipsometry. Financial support from the Rhône-Alpes Region (MIRA program) and french Ecos-Sud de la Recherche (ACI) is also acknowledged.

Notes and references

1 A. C. Templeton, W. P. Wuelfing and R. W. Murray, *Acc. Chem. Res.*, 2000, **33**, 27; J. H. Fendler, *Chem. Mater.*, 2001, **13**, 3196; A. N. Shipway and I. Willner, *Chem. Commun.*, 2001, 2035.
2 D. I. Gittins, D. Bethell, R. I. Nichols and D. I. Schiffrin, *Adv. Mater.*, 1999, **11**, 737.
3 W. Cheng, J. Jiang, S. Dong and E. Wang, *Chem. Commun.*, 2002, 1706.
4 K. Uosaki, T. Kondo, M. Okamura and W. Song, *Faraday Discuss.*, 2002, **121**, 373.
5 Y. Liu, Y. Wang and R. O. Claus, *Chem. Phys. Lett.*, 1998, **298**, 315.
6 Y. Fu, H. Xu, S. Bai, D. Qiu, J. Sun, Z. Wang and X. Zhang, *Macromol. Rapid Commun.*, 2002, **23**, 256.
7 P. Schuetz and F. Caruso, *Colloids and Surfaces A*, 2002, **207**, 33.
8 J. F. Hicks, Y. Seok-Shon and R. W. Murray, *Langmuir*, 2002, **18**, 2288.
9 G. Decher, *Science*, 1997, **277**, 1232.
10 D. Laurent and J. B. Schlenoff, *Langmuir*, 1997, **13**, 1552.
11 J. Hodack, R. Etchenique and E. Calvo, *Langmuir*, 1997, **13**, 2708.
12 E. Forzani, M. A. Perez, M. Lopez Teijelo and E. Calvo, *Langmuir*, 2002, **18**, 9867.
13 N. Ferreyra, L. Coche-Guérente, P. Labbe, E. Calvo and V. Solis, *Langmuir*, 2003, **19**, 3864.
14 Gold colloids were obtained from Sigma (ref. G1402-lot 071K9170 and ref. G1527-lot 092K9183) and contain citrate and tannic acid.
15 P. Mulvaney, *Langmuir*, 1996, **12**, 788.
16 T. Baum, D. Bethell, M. Brust and D. J. Schiffrin, *Langmuir*, 1999, **15**, 866.